https://doi.org/10.5194/egusphere-2025-5639
Preprint. Discussion started: 8 January 2026

Doppler lidar wind profiling: long-term assessment of the perpendicular vertical sweeps reconstruction method

Elsa Dieudonné[1], Pauline Haezebrouck[1], Perrine Maynard[1], Anton Sokolov[1], Hervé Delbarre[1], Patrick Augustin[1], Marc Fourmentin[1]

[1] Laboratoire de Physico-Chimie de l'Atmosphère (LPCA), Université du Littoral Côte d'Opale (ULCO), 59140 Dunkerque, France
Correspondence to: Elsa Dieudonné (elsa.dieudonne@univ-littoral.fr)

Abstract. Doppler lidars have become a relatively common tool to measure wind profiles in the lower troposphere, as commercial instruments improved and became more accessible to answer the demand, notably from the wind energy industry. Most often, the Doppler Beam Swinging (DBS) technique is used to reconstruct the horizontal wind profile from the radial wind raw observations, because it is implemented in the software of commercial Doppler lidars. However, the DBS leaves a blind zone near the ground that makes it difficult to observe very low-altitude phenomena such as certain low-level jets, plus the wind profiles can be noisy if most of the lidar observation time is dedicated to other types of sweeps. However, the horizontal wind can also be reconstructed by combining observations from two vertical sweeps of the Range-Height Indicator (RHI) type, recorded in perpendicular directions. Radial wind observations are binned into horizontal layers, which allows to retrieve both the average wind and its variance, providing an estimation of the horizontal part of the turbulent kinetic energy (TKE). This work introduces a method to take into account the flow inclination over sloping terrains, as well as filter the range-folded echoes from high-altitude clouds. The horizontal wind speed and direction retrieved with this cross-RHI method were compared with standard DBS observations over six months of observations in total, recorded at two urban sites in France, one coastal flat city (Dunkerque) and one continental hilly megacity (Paris). The wind speed intercomparison below 200 m altitude yielded very good correlation coefficients around 0.85 on both sites, with a cross-RHI-*vs*-DBS fitting slope of 0.93. At higher altitudes, up to 3 km, results were even better as range-folded echoes from clouds disappeared from the DBS, with correlation coefficients and slopes both around 0.97 for altitudes above 1 km. The wind direction showed higher dispersion, though in Dunkerque, 83 % of points below 200 m had an error lower than 10°, and 62 % in Paris, where there was no averaging over several DBS cycles. Again, results improved with increasing altitude, demonstrating that the cross-RHI wind reconstruction method can be used to retrieve full-height wind profiles without limiting the sweeps to low-elevation beams. In addition, case studies highlighted the ability of the cross-RHI technique to operate with low aerosol loads, range-folded echoes, and convective conditions. The two-dimensional flow inclination angle could be optimized successfully for about 88 % of the RHI pairs on both sites. The most frequent tilt angle was around 0.6° in Dunkerque and 1.0° in Paris, with 95 % of the values below 8°, though the direction of the steepest slope could only be partially related with the orography. In Paris, the decrease in horizontal TKE permitted by the flow inclination correction was –5.2 % at the lidar level, but could reach –12 % around 1 km altitude, though these values were very sensitive to the altitude band used to optimize the tilt angle. The comparison with a

https://doi.org/10.5194/egusphere-2025-5639
Preprint. Discussion started: 8 January 2026

near-ground ultrasonic anemometer in Dunkerque showed that the cross-RHI retrieval overestimated the horizontal TKE by about 13 %, even when accounting for the flow inclination, though this may result from the slightly higher altitude at which lidar data were recorded.

Short summary. Doppler lidars are now commonly used by the wind energy industry and weather agencies to retrieve vertical profiles of the horizontal wind speed and direction. Commercial instruments rely on the Doppler Beam Swinging technique to reconstruct the wind profile from the raw observations. This study investigates another profiling technique that does not have a blind layer near the ground and is less sensitive to contamination from high-altitude clouds.

1. Introduction

The demand for wind profile observations in the lower troposphere has been steadily growing over the last 30 years, as different types of commercial remote sensing instruments arrived on the market. Weather agencies have built networks of Doppler radars since the 1990's in developed countries such as the USA (Weber et al., 1990) or in Europe (Nash and Oakley, 2001), and middle-income countries such as China are still implementing such networks (Liu et al., 2020). Indeed, assimilating wind profile observations into weather forecast models allows to improve greatly the accuracy and time extent of the forecasts (Benjamin et al., 2004; Smith and Benjamin, 1993; Wang et al., 2020) and only remote sensing instruments can answer the need for continuous and affordable observations. Despite the more recent development of commercial Doppler lidars, Doppler radars are still preferred for weather monitoring networks because they allow to "see" through the clouds and up to the lower free troposphere, while Doppler lidars are blinded by clouds and only provide observations at altitudes where some aerosols are present, i.e. only in the planetary boundary layer (PBL) most of the time. Doppler sodar, the third type of wind remote sensing instrument, shares the radar's ability to pierce through the clouds, but with a more limited range (typically 1.5 km for a sodar, against 2 to 7 km for a radar). However, Doppler lidars are much more compact instruments, that involve much less constraints at deployment than sodars or radars (no need for noise or electromagnetic shielding, or to shelter the instrument's electronics in a nearby building). Doppler lidars also offer a great versatility in terms of scanning strategy (as the laser beam can be oriented using only small rotating mirrors). Therefore, and despite their limited range, Doppler lidars have become the most common type of instrument employed for applications out of weather monitoring networks.

The wind energy industry is another sector that pulled the growing demand for remote-sensing wind profile observations, in the wake of the fast development of wind farms since the 2000's. With the increase of the turbine size over time, using meteorological masts to obtain wind observations at the hub height has become virtually impossible, making Doppler lidars necessary to evaluate the production potential of a future wind farm site (Emeis et al., 2007). Wind profile observations are also essential to improve the accuracy of the near real-time models used to pilot the turbines, in order to adjust the electricity production to the demand or to limit the turbine fatigue in case of strong wind shear (e.g. Dolatabadi et al., 2022; Theuer et al., 2020). Aviation safety is another domain where wind profile observations proved very useful (Thobois et al., 2019), notably

https://doi.org/10.5194/egusphere-2025-5639
Preprint. Discussion started: 8 January 2026

helping to secure landings and take-offs by warning the pilots from brutal changes in the headwind, and thus the plane airlift. After the pioneering work performed in Hong Kong in the early 2000's (Shun and Chan, 2008), major airports throughout the world have been equipped with Doppler lidars to provide real-time alerts for low-altitude wind shear (e.g. Hong Kong Observatory, 2019). Finally, in atmospheric research, field campaigns dedicated to pollution dispersion, desert dust transport, surface-atmosphere exchanges or cloud formation now commonly include wind profile observations, that are a powerful tool to interpret gas or particle observations (e.g. Chazette et al., 2021; Crumeyrolle et al., 2019).

Wind profile reconstruction methods and the underlying scanning strategies were first developed for Doppler radars, and then passed to Doppler lidars. Originally, wind profiles were reconstructed using the Velocity Azimuth Display (VAD) method, where the beam performs a conical sweep at a fixed elevation from the ground, called a Plan-Position Indicator (PPI) scan (Browning and Wexler, 1968). Radial wind observations along the "ring" located at a given altitude are fitted, generally using a sinusoidal function, to retrieve the horizontal wind speed and direction. The VAD method was then simplified into the Doppler Beam Swinging (DBS) method, where the continuous conical sweep is replaced by only two or four slant beams oriented towards perpendicular directions (Clark et al., 1985). The horizontal wind speed and direction are retrieved through linear combination of the radial wind along the different beams, with an additional vertical beam to retrieve the vertical wind component. The DBS is the most commonly used wind reconstruction method nowadays because it is included in the built-in software of the commercial instruments. Recent developments concern the retrieval of the covariances between the 3-dimensional wind components that are necessary to derive the turbulent momentum fluxes, which can be done using the six-beam method (Sathe et al., 2015). Upgrades to the VAD technique with more complex data processing methods have also been proposed, in order to extend its vertical range into the free troposphere (Baidar et al., 2023).

However, the DBS and six-beam methods share a common limitation: the wind cannot be retrieved in the lowest layers of the PBL, corresponding to the blind zone common to of all types of remote sensing instruments. For Doppler lidars and sodars, the blind zone is at least 40 or 50 m deep – more for radars – which may be problematic for meteorological studies (e.g. regarding low-level jets) or for pollution applications (e.g. to characterize the dispersion from ground-level sources). In urban areas especially, the instrument must generally be installed on a building to avoid obstacles blocking the slant beams, so the blind zone depth is increased by the station altitude above ground level. The wind profile can of course be extended downwards using anemometers, but deploying a meteorological mast is not always possible, especially in urban areas, not mentioning it is more convenient and less expensive to use a single instrument to retrieve the whole profile. Besides, DBS wind profiles may be noisy when only a reduced number of consecutive cycles are recorded, which is the case when the measurement scenario must include other types of scans, e.g. horizontal sweeps to visualize turbulent coherent structures (Cheliotis et al., 2020; Maynard et al., 2025) or vertical sweeps to monitor the progression of a front (Augustin et al., 2020; Wakimoto et al., 2006). If the observed phenomenon requires other types of scans with a high repetition rate, the number of DBS cycles will necessarily be limited, and the six-beam method will not be applicable, as it requires continuous observations over typically half-hour averaging periods. Additionally, operating a scanning lidar continuously in the DBS or six-beam configuration causes increased fatigue on the periscope gears, as the latter will rotate at full speed in-between the beams, much faster than during a

https://doi.org/10.5194/egusphere-2025-5639
Preprint. Discussion started: 8 January 2026

conical or vertical sweep (with the lidar used in Dunkerque for this study, the gears started grating after a few weeks of continuous DBS operation, which was not improved by lubricating them).

Considering the blind zone problem, the lowest atmospheric layers can be sampled only using low-elevation beams, in which case the horizontal distance between opposite beams of a DBS or six-beam cycle would become too large to reasonably assume horizontal homogeneity of the wind in the sampled volume, especially in a convective PBL (Céspedes, 2024). The VAD method still works at low elevations because it relies on a much larger number of beams, and the sinusoidal fit allows to separate the contribution of turbulence from the mean wind. Another way to observe the low-altitude wind is to use vertical sweeps of the Range-Height Indicator (RHI) type. Such scans have been used since the 2000's with Doppler lidars to monitor low-altitude wind shear and airplane wake above airports' runways (Shun and Chan, 2008), and with both lidars and radars or to observe the progression of a front (Augustin et al., 2020; Wakimoto et al., 2006). To obtain the two components of the horizontal wind, it is necessary to combine two RHI sweeps in perpendicular (or sufficiently different) directions. The two scans can be recorded successively by the same instrument, or simultaneously by two instruments located a few kilometres apart (Calhoun et al., 2006; Chong et al., 2000; Newsom et al., 2005). The second approach, called dual-Doppler, is expensive and complex to implement as it requires two instruments with similar performances, positioned at roughly the same altitude and synchronized in time.

In this article, we consider the first approach, that we can name single-Doppler cross-RHI technique. The associated wind reconstruction method, which consists in binning the data into horizontal layers, was introduced by Banta et al. (2002) to observe a low-level jet close to the ground (in this first study, observations from PPI and RHI scans were merged in the retrieval process). The single-Doppler cross-RHI technique also has the advantage to provide the horizontal wind variance profile, thus opening for turbulence studies (Banta et al., 2006). To our knowledge, this technique has only been reused once since then, when Bonin et al. (2017) compared it to other wind and turbulence profile-reconstruction methods (VAD and six-beams) and ultrasonic anemometer measurements on a 300-m mast. These two studies limited the elevation of the RHI scans to ~45° to safely neglect the contribution of the vertical wind, which limited the extension of the reconstructed profile to ~600 m. Also, only a few days of data were used in these two studies, so more evidence is still needed to validate the single-Doppler cross-RHI technique over a longer period and in more varied conditions. Finally, this method was only applied to very flat plain sites, where the air flow is fully horizontal; its applicability in cases when the flow layers are visibly inclined has not yet been explored.

This article has therefore two objectives: *(i)* to propose a comprehensive validation of the horizontal wind profiling from the cross-RHI technique and *(ii)* to introduce a method to account for the air flow inclination and assess its impact on the Turbulent Kinetic Energy (TKE) retrieval. To validate the horizontal wind retrieval, a comparison with standard DBS wind profiles will be performed on a much longer time period (six months in total), on two sites that experience varied meteorological conditions: Dunkerque, a coastal flat site on the North Sea shore, and Paris, an inland site with hills and a large river (both in France). The comparison will bear on full-height wind profiles derived from RHI scans reaching the zenith, to assess if the single-Doppler cross-RHI technique can completely replace the DBS technique that is currently implemented by default in commercial

https://doi.org/10.5194/egusphere-2025-5639
Preprint. Discussion started: 8 January 2026

Doppler lidars. Regarding, the air flow inclination correction, different configuration of the tilt angle optimization process will be discussed, and near-ground TKE observations will be compared with an ultrasonic anemometer for the Dunkerque site. Section 2 will therefore present the instrumentation, the Dunkerque and Paris datasets and the data processing steps, while Section 3 will provide the results of the intercomparison with the DBS method and expose the effects of the flow inclination correction. Finally, Section 4 will conclude about the reliability of the single-Doppler cross-RHI technique and its applicability to derive full-height and blind-zone-devoid wind and TKE profiles, even in sloping sites.

2. Dataset and methodology

2.1. Instruments and observations

The wind profile reconstruction method proposed in this article was tested on observations recorded on two different sites (Table 1), using two different scanning Doppler lidars from the Leosphere/Vaisala company (Saclay, France). Dunkerque is a 200,000-inhabitants industrial harbor city on the North Sea coast, surrounded by a flat topography. As a coastal site, Dunkerque experiences many dynamic phenomena, such as sea breezes, wind channeling in the nearby Dover Strait and storms (Dieudonné et al., 2023). In Dunkerque, the lidar was installed in the port, ~1.6 km from the shoreline, on the belvedere of the 'Halle aux Sucres' building (51.037511°N, 2.365979°E, ~15 m above ground level). The Doppler lidar used in Dunkerque was a Scanning Wind Cube WCS200 acquired in 2022. Four months of data recorded from July 20th to November 19th were used to compute statistics on the performances of the cross-RHI wind retrieval method . Results from the megacity of Paris will also be presented, to show how the wind profile reconstruction method performs in the presence of moderate orography (hills of ~100 m height) and with an older instrument. In Paris, the lidar was installed in the very center of the city, near the Seine river, atop of the main tower of the Jussieu campus of Sorbonne University (48.84693°N, 2.355435°E, ~75 m above ground level). The Doppler lidar was a Scanning Wind Lidar WLS100 acquired in 2013. The observations presented in this article are part of the 2-month dataset recorded from September 4th to November 6th 2014 in the framework of the VEGILOT campaign and used in the studies of Cheliotis et al. (2021, 2020) about coherent turbulent structures.

https://doi.org/10.5194/egusphere-2025-5639
Preprint. Discussion started: 8 January 2026

Table 1. Observation sites, characteristics of the Doppler lidars instruments used in this study and parameters of the measurements. The duration of the measurement scenario is the time after which each type of sweep (DBS or RHI) was repeated; other types of scans were included, so the total duration exceeds the sum of the RHI plus DBS duration.

Observation site	Name	Dunkerque	Paris
	GPS coordinates	51.037511°N, 2.365979°E	48.84693°N, 2.355435°E
	Ground / instrument altitudes	7 m / 15 m	35 m / 75 m
	Site environment	Coastal, urban/industrial, flat plain	Continental, urban (megacity), river + hills
	Observation dates	July 20th – Nov. 19th 2023	Sept. 4th – Nov. 6th 2014
Doppler lidar Instrument	Model (both from Leosphere/Vaisala)	Scanning Wind Cube WCS200	Scanning Wind Lidar WLS100
	Wavelength	1.543 µm	
	Pulse repetition frequency	40 kHz at 25 m axial resolution, 20 kHz at 50 m	
	Accumulation time	1 s per beam	
Measurement scenario	Total duration	15 min. 40 s	20 minutes
	Number of cycles	10,426	4,580
DBS sweeps	Number of cycles / duration	10 / 2 min. 30 s	1 or 2 / 30 s
	Beams' azimuth / elevation	0°/75°, 90°/75°, 180°/75°, 270°/75° + n.a./90° in Dunkerque	
	Vertical resolution / blind zone	25 m / 0 to 50 m	50 m / 0 to 100 m
	Maximum theoretical height	3.3 km	5.0 km
RHI sweeps	Beam azimuth	0° (North to South), 90° (East to West)	
	Elevation range / step	0° to 180° / 2°	
	Range resolution / blind zone	25 m / 0 to 50 m	50 m / 0 to 100 m
	Maximum theoretical range	3.3 km	5.0 km
	Duration	90 s per sweep, ~3 min. 10 s for the pair	

The measurement scenario was not the same in Dunkerque and in Paris, but both sequences included vertical sweeps of the RHI type, in two perpendicular directions: North-South (azimuth 0°-180°), then East-West (azimuth 90°-270°). All the RHI sweeps had a resolution of 2° in elevation, from ground (0° elevation) to ground in the opposite direction (180° elevation). Given the accumulation time of 1 s per beam, a pair of cross-direction RHI sweeps took a bit more than 3 minutes to record. The range resolution of the RHI sweeps on both sites was 25 m, with a maximum range of 3.3 km and a blind zone of 50 m at close range. About four pairs of cross-RHI sweeps per hour were recorded in Dunkerque, but only three in Paris. The measurement scenario in both cities also included wind profiles using the reference DBS method. In Paris, the DBS cycle

https://doi.org/10.5194/egusphere-2025-5639
Preprint. Discussion started: 8 January 2026

included only four slanted beams in the cardinal directions, with an elevation of 75° (15° from zenith), while in Dunkerque, a fifth vertical beam was added. Besides, only one or two consecutive DBS cycles were recorded in Paris, while ten cycles were recorded in a row in Dunkerque, the wind profile being average over these cycles. Therefore, the DBS wind profiles recorded in Paris were noisier than those recorded in Dunkerque. Also, the DBS vertical resolution differed on the two sites – 25 m in Dunkerque and 50 m in Paris – so that the blind zone was also different – 50 m-deep in Dunkerque, but 100 m in Paris (above the instrument).

In Dunkerque, the low-altitude TKE retrieved by the lidar could be compared with the observations from a 3-dimension ultrasonic anemometer (Metek USA-1 "Scientific" from Metek GmbH, Elmshorn, Germany). The anemometer was settled near one of the port's lock, atop a 15-m mast located ~1.4 km North from the Doppler lidar and at the same altitude above ground and sea level. The anemometer operated at a 20 Hz frequency, turbulence parameters were computed online from the raw data over 15-minute periods, and only the averaged data were stored.

2.2. Data filtering

For all types of sweeps, individual data points were filtered using a threshold on the Carrier-to-Noise Ratio (CNR): a minimum value of −27dB was required to retain the wind observations, as advised by the lidar manufacturer. A second threshold was applied on the 'radial wind dispersion'; this parameter describes the dispersion of the scattering particles' speed in the atmospheric volume occupied by the laser pulse and is derived from the peak half-height width in the Doppler spectrum. A maximum value of radial wind dispersion of 2.9 $m.s^{-1}$ was imposed to retain the wind observations, as the manual inspection of the data revealed that a common and perfectly identical value of 2.92 $m.s^{-1}$ was always associated with spurious points produced by the instrument itself (and not due to atmospheric phenomena such as clouds). Additionally, radial wind values falling out of the observation range indicated by the manufacturer (± 30 $m{\cdot}s^{-1}$) were filtered out.

For the RHI only, a two-dimensional filter was applied to remove isolated points in the sweep: only points having at least three neighbors with good-quality observations were retained (here, neighbors were defined in the sweep polar coordinates, i.e. the previous/next elevation value and the previous/next range value). This filter was added because the manual inspection of the data revealed that isolated data points were often associated with aberrant wind values, but it also proved efficient to remove part of the range-folded echo cases. A range-folded echo appears when an elevated cloud is located farther than the lidar maximal range, so that the light backscattered by the cloud returns to the lidar after the next laser pulse has been emitted. The signal from the elevated cloud thus adds to the signal from a lower-altitude air layer, and is usually associated with a much higher wind value, as can exist in the free troposphere. The fold signal from a horizontal cloud layer will form a 'whiskers' pattern on the RHI sweep image (Fig. S1.a of the supplement). The isolated-point filter removed the fold signal for cases when it appeared in a layer devoid of clean-air signal (Fig. S1.b).

https://doi.org/10.5194/egusphere-2025-5639
Preprint. Discussion started: 8 January 2026

2.3. Wind profile reconstruction

The horizontal wind retrieval process can be divided into three steps: firstly, the radial wind is converted into one of the horizontal wind components (zonal or meridional, Sec. 2.3.1); secondly, the horizontal wind components are averaged over atmospheric layers (Sec. 2.3.2); and thirdly, the horizontal wind components are combined to reconstruct the horizontal wind (Sec. 2.3.3). In the first two steps, each RHI sweep is processed separately, and the two cross-RHI of a pair are combined in the third step.

2.3.1. From radial to horizontal wind

The radial wind from a DBS or from RHI sweeps recorded in the cardinal directions depends on one of the horizontal wind component (zonal or meridional) and on the vertical wind (Figure 1). In the DBS retrieval, the contribution of the vertical wind is canceled by linear combination of the two beams recorded in opposite directions, supposing that the vertical wind is the same along both beams, at a given altitude. This hypothesis of horizontal homogeneity in the wind field is justifiable in the free troposphere or in the residual layer, where the large-scale motion dominates, but not in the turbulent boundary layer. Additionally, convective motions may be associated with vertical wind speeds of a few meters per second, comparable in magnitude with the horizontal motion, so that the poor correction of w in the DBS retrieval may produce apparently 'noisy' results for u and v in the convective boundary layer. Usually, time averaging is used to compensate for this effect, by recording series of consecutive DBS profiles, but this possibility is limited when the measurement scenario has to include other types of sweeps, for instance horizontal ones to observe turbulent structures.

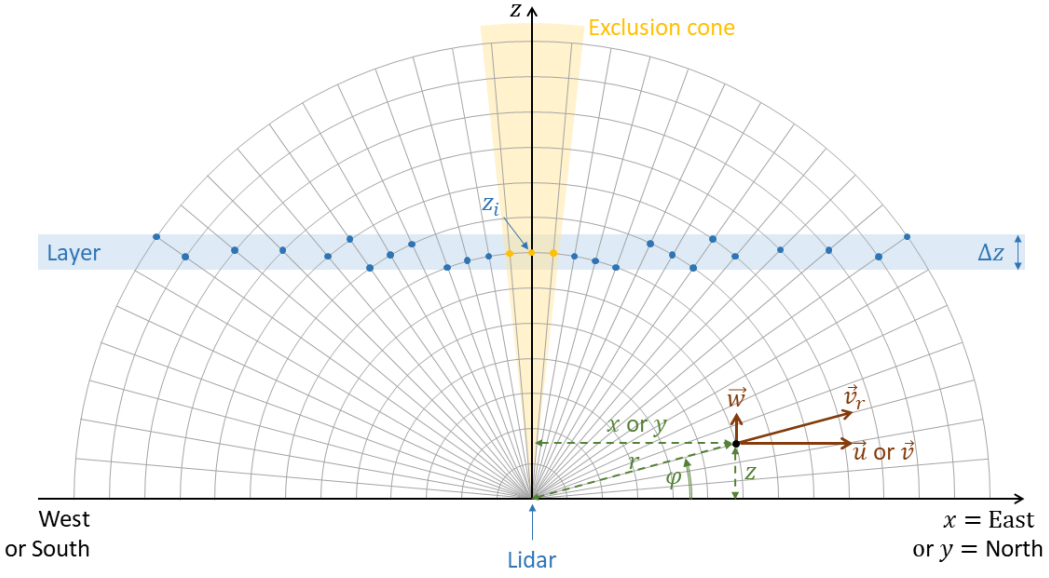

Figure 1. Scheme of a RHI sweep showing part of the data grid points (grey lines), the radial wind vector for a given point along with its components (brown arrows) and the polar and Cartesian coordinates of this point (green). The wind average and standard deviation over the horizontal layer of depth Δz centred over altitude z_i (blue shading) are computed on the grid points belonging to the layer (blue dots), except the points located in the exclusion cone around the zenith (yellow shading and dots).

https://doi.org/10.5194/egusphere-2025-5639
Preprint. Discussion started: 8 January 2026

In the cross-RHI profiling method, the choice is instead *(i)* to exclude the beams for which the contribution of the vertical wind cannot be reasonably neglected, and *(ii)* to replace the time averaging by space averaging in horizontal layers. Regarding the first point, the too-vertical beams were excluded, using an empirical threshold of 0.2 on the cosine of the elevation (counted from the ground), i.e. a 12°-half-width cone around zenith (Figure 1). This limit can be adjusted depending on the observation site; continental or tropical atmospheres experiencing vigorous convective motions may require a wider exclusion cone around zenith, at least during daytime. The horizontal wind components are then computed from the radial wind assuming the vertical wind contribution is negligible.

2.3.2. Averaging in atmospheric layers

In the main step of the reconstruction process, the RHI sweep is divided into horizontal layers, and the average and variance of the horizontal wind are computed in each layer, to compose the vertical profile of the zonal or meridional wind component. In this study, the layers' central altitude and depth were set to match the DBS profiles, with the aim to facilitate the intercomparison. In Dunkerque, this choice also minimized the difference in height between the ultrasonic anemometer and the RHI lowest reconstruction layer, which had a central altitude of zero (i.e. at the lidar level). As a consequence, the depth of this layer was equal to the half of the other layers' depth.

As a last data filtering step, outlier wind values falling out of the ±3σ-interval in each layer were discarded before computing the wind statistics. This allowed to filter the range-folded echoes for which the spurious points were located amongst good-quality wind observations (Fig. S1.c), based on the fact that the wind values from the fold signal are generally much stronger as they correspond to the free troposphere. Besides, the wind statistics were computed only in the layers where at least 30 data points remained after the outlier filtering step. Due to this threshold, the maximum theoretical altitude of the reconstructed profile was 2.9 km in Dunkerque, for ground-to-ground RHI sweeps with a maximum range of 3.3 km and a 25-m axial resolution. The typical number of good-quality data points was around 150 in the lowest layer, and close to 230 in the other layers below 0.5 km (Fig. S8b and S9f). As for the DBS technique, the effective maximal range of the cross-RHI reconstructed profile corresponds most of the time to the boundary layer top altitude, as the aerosol load in the free troposphere is usually too low to maintain the CNR above the −27 dB threshold.

Maintaining a sufficient level of CNR is also necessary for the contribution of the measurement error to the standard deviations to remain negligible. Indeed, the radial wind measured by Doppler lidar includes a random measurement error coming from the shot noise, from an imperfect laser frequency control, from the random movement of the scattering particles etc. This random error cancels when computing the average wind components, but results in an additional term of error variance when computing the standard deviations. Eberhard et al. (1989) estimated the random error by computing the wind measurements obtained when shooting at a fixed target. As no method has been proposed to correct the random error contribution in the cross-RHI reconstruction method, other authors (Banta et al., 2002; Bonin et al., 2017) simply neglected this error's contribution, an assumption that is valid only if the level of CNR is high enough. With a lidar identical to the one used in Dunkerque, Bonin et al. (2017) concluded that the manufacturer's threshold at −27 dB was sufficient.

https://doi.org/10.5194/egusphere-2025-5639
Preprint. Discussion started: 8 January 2026

2.3.3. Reconstructing the horizontal wind

The horizontal wind speed and direction are computed from the zonal and meridional wind components using the same formula as for the DBS wind reconstruction. If the RHI sweeps are not oriented towards the cardinal directions (for instance because there are obstacles blocking the low-altitude beams in these directions), but the two RHI sweeps are still perpendicular to one another, the azimuth of the first sweep of the pair must simply be added as an offset to the wind direction. To avoid obstacles, it is also possible to use non-perpendicular RHI sweeps, which modifies the wind reconstruction formulas (Sec. S2 of the supplement). Studies about Dual-Doppler configuration have investigated what value the minimum angle between the two beams should have to maintain a tolerable level of error on the reconstructed wind. Davies-Jones (1979) recommended a minimum angle of 30°, and we can assume the same applies to the cross-RHI method. A last solution to avoid obstacles can be to use half-RHI sweeps (from ground to zenith). This will reduce the maximal range and make the retrieval more sensitive to low-aerosol loads (as it divides by two the number of points included in each layer).

2.3.4. Turbulent kinetic energy

The meridional and zonal wind variances can be used to compute the horizontal part of the TKE, or TKE_h. The full TKE can only be retrieved if the lidar measurement scenario includes series of vertical shots (i.e. vertical Line Of Sight or LOS) for at least a minute, which was unfortunately not done during the period used in this comparison study. However, the horizontal TKE can still be useful, for instance to determine the nocturnal boundary layer height, that can be difficult to distinguish using a ceilometer or an aerosol lidar, as particles are present both in the nocturnal boundary layer and in the residual layer just above.

The horizontal TKE retrieved from a remote sensing lidar instrument differs from the one measured using an in-situ ultrasonic anemometer for several reasons, the main ones being volume averaging and beam recombination effects (Sathe and Mann, 2012). Volume averaging denotes the fact that Doppler lidars do not measure the wind at a precise point, but within the air volume occupied by the laser pulse, which makes eddies smaller than the range resolution indiscernible. Beam recombination effects refer to the consequences that the air mass displacement during the sweep has, when it comes to combining the beams at the data processing step. For instance, Sathe and Mann (2012) showed than beam combination in DBS profiling resulted in overestimating the energy in the intermediate part of the spectrum. For partial RHI sweeps (up to 45°), Bonin et al. (2017) observed that the TKE tended to be overestimated during low-turbulence periods, compared with ultrasonic anemometers. One of the possible explanation they gave was an artificial increase of the variances of the horizontal wind components due to the flow inclination, which will be addressed in the next section.

2.4. Accounting for the flow inclination

RHI scans recorded in Paris, and to a lesser extent in Dunkerque, have been observed to exhibit a small, but visible inclination of the flow (Fig. S3.a). To take this into account, an offset must be added to the elevation of the beams, from the very beginning

https://doi.org/10.5194/egusphere-2025-5639
Preprint. Discussion started: 8 January 2026

of the wind reconstruction process. The so-called horizontal wind speed in Sec. 2.3.1 thus becomes a quasi-horizontal wind speed computed following a plane slightly tilted from the horizontal. Then, the layers in which the wind is averaged are tilted by the same offset. The proper offset value to use is the one that minimizes the wind variability inside the layers. Indeed, if the averaging layers follow the flow inclination, the quasi-horizontal wind values inside a given layer will have very close values. Conversely, if the averaging layers are tilted from the flow direction, the quasi-horizontal wind values inside a given layer will vary due to the vertical wind shear. Obviously, the optimal offset value will be different for the two RHI orientations and is not expected to be constant in time, so that it must be determined separately for each RHI scan as part of the retrieval process. In order to determine the proper inclination angle for the averaging layers, it is necessary to define an "error" ε, i.e. a one-dimensional function of the offset angle, that can be minimized using a numerical optimization process. Here, the error was defined as the average wind variance in the layers from the lowest part of the profile (more details are provided in Sec. S3.1 of the supplement). Different configurations were tested, with the error being computed using the lowest 0.5, 1.0, or 1.5 km of the profile. This choice does not affect the horizontal wind reconstruction, but its effect on the horizontal TKE retrieval will be discussed in Sec. 3.2.2.

Figure S3(c) presents an example of error curve, with the result of the optimization process. The minimum was found using the MATLAB® function `fminbnd`, which algorithm is based on golden section search and parabolic interpolation (Brent, 1973; Forsythe et al., 1976). This method was preferred because of its robustness, i.e. its ability to converge toward the absolute minimum and not a local minimum, and because it can be parametrized to force the search to start by a zero tilt angle, though this results in an asymmetric search interval around zero. Details about the parametrization of the optimization function and the inclination search interval are given in in Sec. S3.2 of the supplement. In practice, the minimum of the error function was well defined when the PBL was sufficiently stratified, i.e. during night-time. Conversely, for RHI scans recorded in a strongly convective PBL (Fig. S3.b), the error function did not always present a minimum (Fig. S3.d). In this case, no optimization was performed and the wind profile was retrieved without inclination of the averaging layers.

When the optimization was performed successfully for the two RHI scans of a pair, the doublet of layers' inclination angles, retrieved respectively in the zonal and meridional directions, was combined into a two-dimensional flow inclination (Sec. S3.3 of the supplement). The latter was characterized by the azimuth of the steepest slope direction and the inclination of the plane in this direction, to make the geophysical interpretation easier.

3. Results and discussion

3.1. Cross-RHI to DBS intercomparison

3.1.1. One-day case studies

Figure 2 presents the results of the cross-RHI and DBS horizontal wind reconstruction methods for a late summer day in Dunkerque (September 9th 2023), during which particles were present in the free troposphere up to 3 km altitude, extending

https://doi.org/10.5194/egusphere-2025-5639
Preprint. Discussion started: 8 January 2026

the effective range of the Doppler lidar. Both reconstruction methods allowed to identify the same two main air masses: the boundary and residual layers (up to 0.5 to 1.0 km altitude) belonged to a slow continental air mass for the south-east, while the free troposphere above consisted in a faster oceanic air mass from the south-west. Additionally, a north-north-westerly sea breeze developed after 11:30 UTC in the lowest 200 m above ground, then progressively turned into an east-north-easterly land breeze after sunset (around 18:20 UTC).

The white line at the bottom of Figure 3(b, d) corresponds to the 50-m deep blind zone of the DBS observations. Filling in this gap allows to properly observe the onset of the sea breeze or the decay of the land breeze, that are fully visible on the cross-RHI reconstruction (Figure 3c), but missing on the DBS reconstruction (Figure 3d) as the breeze layer was too shallow at these times. Besides, the DBS reconstruction produced missing data in two small layers around 200 and 300 m altitude, from 02:00 to 07:00 UTC (Figure 3b, d). In these layers where the air was cleaner, the CNR values were close to the −27 dB threshold, so that part of the radial wind data was missing. For the DBS method, a single missing observation on one the four slant beams at a given altitude impedes the horizontal wind reconstruction at this altitude whereas the cross-RHI method is much less sensitive, given that the reconstruction of each wind component relies on about 230 points in each layer. Conversely, only the DBS retrieval provided wind values above 2.6 km, as the RHI layers contained less good-quality data points than the required minimum.

Two other one-day examples are shown in Sec. S4 of the supplement, for the inland site of Paris. Figure S7 presents an autumn day that even better illustrates the higher ability of the cross-RHI method to retrieve the horizontal wind with a low aerosol content in the atmosphere, and the interest to fill in the blind zone. In Paris, the lidar was installed on a tall tower to perform horizontal sweeps without obstacles, and the lidar parameterization resulted in a 100-m deep blind zone, so that the lowest point of the DBS profile was located almost 200 m above ground. The cross-RHI reconstruction method thus allowed to better characterize phenomena such as nocturnal low-level jets, without giving up on the horizontal sweeps dedicated to turbulence studies. Finally, Fig. S9 presents a late summer day that illustrates the performance of the two wind reconstruction methods in a strongly convective PBL. The cross-RHI method produced smoother, less noisy results than the DBS method with a measurement scenario in which the time reserved for DBS sweeps was limited.

https://doi.org/10.5194/egusphere-2025-5639
Preprint. Discussion started: 8 January 2026

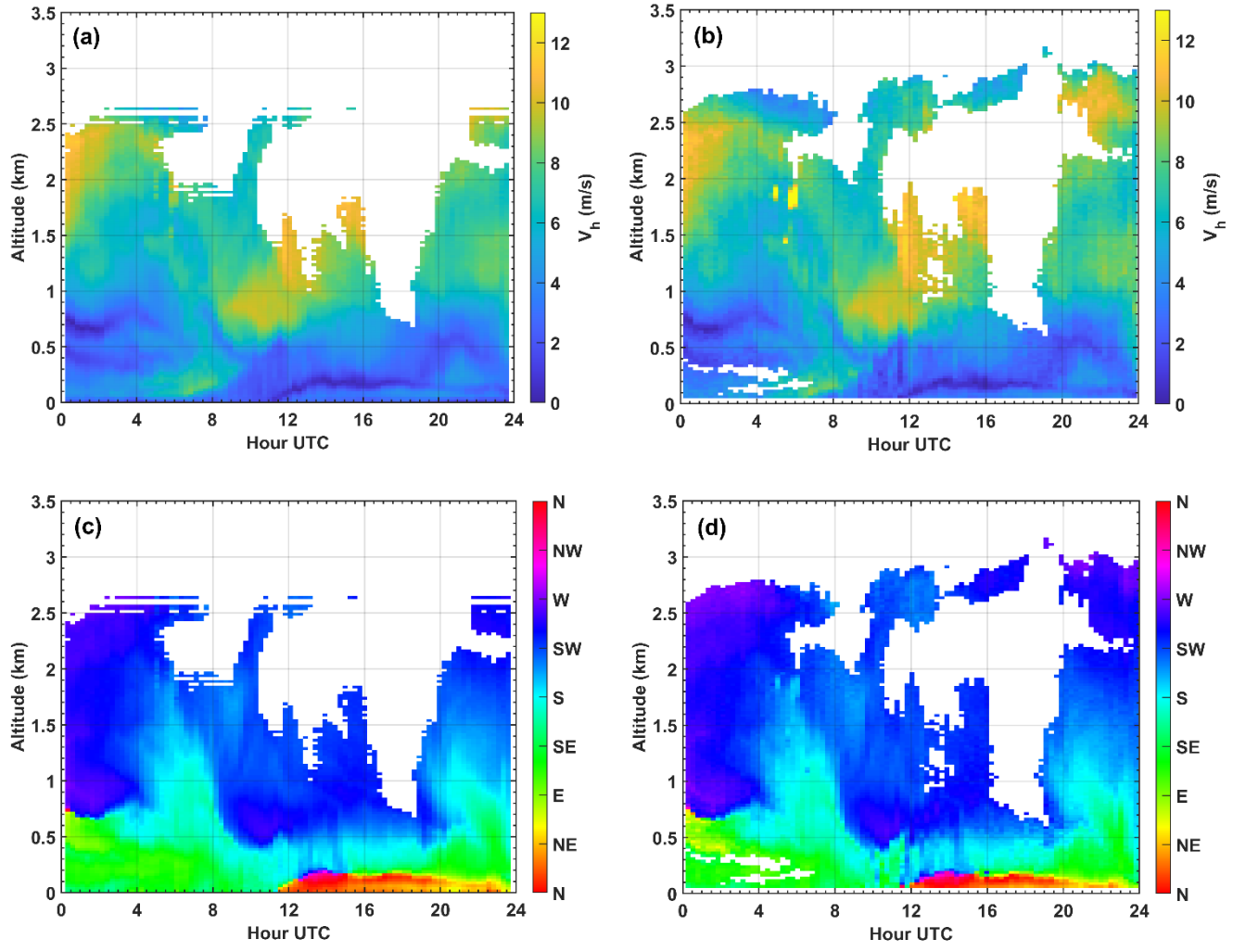

Figure 2. Time-altitude cross-section of the horizontal wind speed (a, b) and direction (c, d) retrieved over Dunkerque on September 9th 2023 using the cross-RHI method (a, c) and the DBS technique (b, d). The colour scales are identical for the two wind speed and the two wind direction panels, respectively.

3.1.2. Statistical validation

Figure 3 illustrates the global intercomparison between the horizontal wind speed values retrieved using both reconstruction methods, gathering data from the whole intercomparison periods and for all altitudes between the top of the DBS blind zone (50 m in Dunkerque, 100 m in Paris) and 200 m above the lidar. This represents a total of 53,667 measurement points in Dunkerque (Figure 3a) and 11,248 points in Paris (Figure 3b). In Dunkerque, the speed difference was less than 10 % for 65 % of the observations (i.e. points located between the 0.9:1 and 1.1:1 lines). The dispersion was higher in Paris, with only 45 % of the observations having an error below 10 %, but this was expected as the DBS observations were noisier in Paris for not being averaged on several cycles as in Dunkerque. Nevertheless, the agreement remained very good on both sites, with a

https://doi.org/10.5194/egusphere-2025-5639
Preprint. Discussion started: 8 January 2026

high Pearson correlation coefficient of 0.86 in Dunkerque and 0.84 in Paris. Data were fitted using an orthogonal regression (adapted for cases where the x and y variables have a symmetric role) that returned slopes values close to one (0.93 at both sites) with small intercept values (+0.36 $m \cdot s^{-1}$ in Dunkerque and +0.21 $m \cdot s^{-1}$ in Paris).

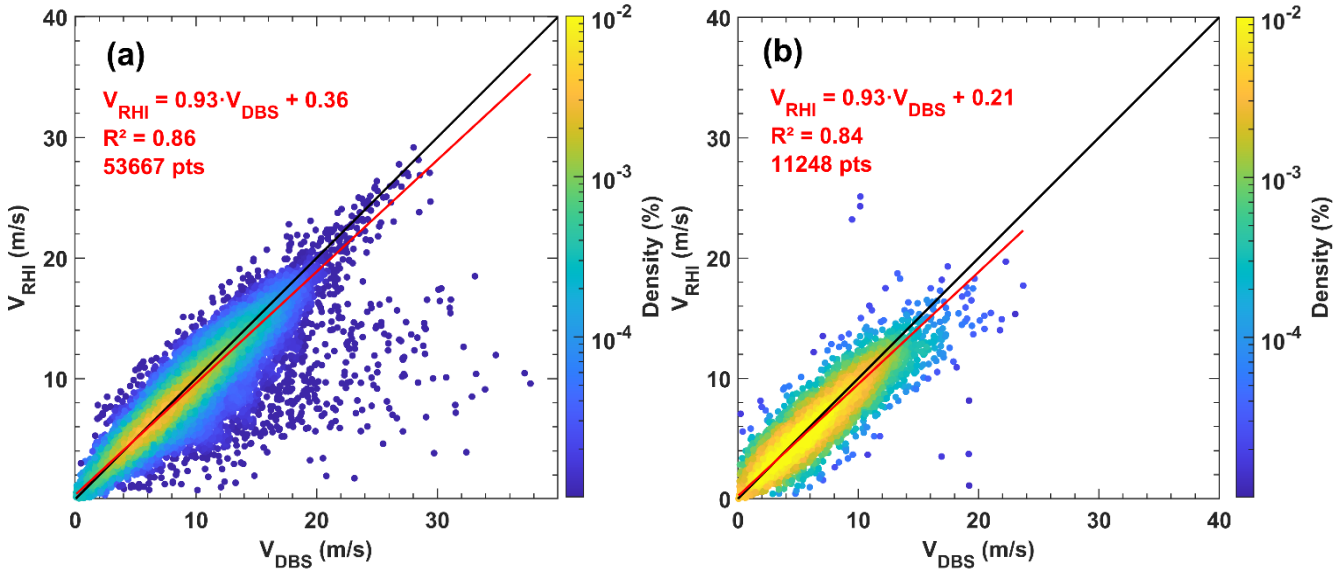

Figure 3. Scatter plot of the horizontal wind speed values retrieved by the DBS technique *vs* the cross-RHI method in (a) Dunkerque and (b) Paris. For each site, the figure includes data from the whole period indicated in Table 1, and for all altitudes between the top of the DBS blind zone and 200 m above the lidar. The black and red lines represent the 1:1 line and the result from the orthogonal regression respectively. The colour scale represents the density of points, expressed as a fraction of their total number, in log scale.

Despite the fact that the clouds of points appear at first sight to be well-centered around the 1:1 lines, the slope values were slightly lower than one, indicating a tendency of the DBS to produce higher wind speed values. In Dunkerque, the slope was drawn by a small share of points for which the DBS speed values were much higher than the cross-RHI speed values. An example of such points can be seen on Figure 2(a, b), around 1.8 km altitude and between 05:30 and 06:00 UTC; the wind speed values reached almost 19 $m \cdot s^{-1}$ on the DBS but were only around 9 $m \cdot s^{-1}$ on the cross-RHI retrieval. The time and height continuity of the wind speed values retrieved by the cross-RHI method being much more plausible, the DBS retrieval was most probably faulty. On this day, like for the other cases of gross overestimation from the DBS retrieval, we suspect that range-folded echoes were responsible. Indeed, range-folded echoes are impossible to filter from the DBS observations, contrary to the RHI where the space continuity with the other points in the sweep can be used (Sec. 2.2). Fluctuations from turbulence could also be suspected, but they would yield both over and underestimation of the wind speed on the DBS retrieval, while only gross overestimation points are visible on Figure 3(a).

The statistical intercomparisons of the wind speed values in higher altitude bands, up to 3 km, are presented in Sec. S5.1 of the supplement. In Dunkerque, the fraction of points with a speed difference lower than 10 % reached ~75 % between 200 and 1,000 m above the lidar, and even ~80 % above 1,000 m. In Paris, the share of observations having an error <10 % also rose with increasing altitude, but the dispersion remained higher than in Dunkerque (61 % for the 200-500 m altitude band, ~69 %

https://doi.org/10.5194/egusphere-2025-5639
Preprint. Discussion started: 8 January 2026

between 500 and 1,500 m and ~78 % between 1,500 and 2,500 m). Consequently, on both sites, the slope values were closer to one in elevated layers (typically 0.97), and the intercept values were smaller (typically < 0.1 m·s^{-1}, Fig. S10), with Pearson correlation coefficients always above 0.91, and even 0.96 above 1,000 m. Indeed, the number of points for which the DBS retrieval returned much larger values than the cross-RHI method decreased with increasing altitude. This is likely because the clouds that cause range-folded echoes on the DBS sweeps are not the same types for low-altitude and high-altitude echoes. Low-altitude echoes are caused by mid-level dense liquid water clouds, while high-altitude echoes are causes by high-level optically-thin ice crystal clouds. The signal returned by the second type of clouds is less intense, so that the peak in the Doppler spectrum corresponding to the wind speed in the cloud is less susceptible to be mistaken with the peak resulting from the low-altitude wind.

Figure 4 illustrates the global intercomparison between the horizontal wind direction values retrieved using both reconstruction methods by gathering, like in Figure 3, data from the whole intercomparison periods and for all altitudes between the top of the DBS blind zone and 200 m above the lidar. Again, the agreement was very good in Dunkerque, with 61 % (resp. 83 %) of the observations for which the direction difference was less than 5° (resp. 10°), while there was more dispersion in Paris, where the corresponding numbers were only 39 % (resp. 62 %) due to the lack of averaging on several DBS cycles. Besides, the differences appeared to behave alike in all the wind directions (Figure 4). Similar results were obtained for the higher altitude bands: as for the wind speed, the number of points corresponding to large differences between the cross-RHI and DBS retrievals decreased with increasing altitude (Fig. S11). Consequently, the fraction of data with a direction difference <5° (resp. <10°) increased with increasing altitude: it was above 77 % (resp. >91 %) for altitudes >1 km in Dunkerque, while it reached 64 % (resp. 81 %) between 500 and 1,500 m in Paris.

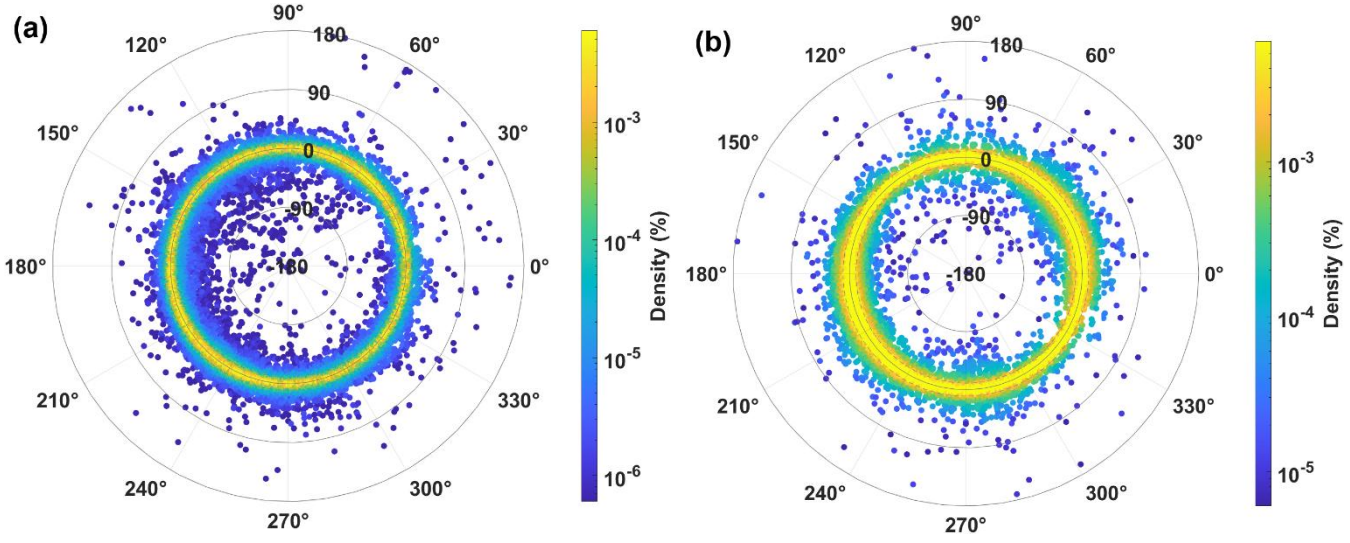

Figure 4. Horizontal wind direction difference (cross-RHI minus DBS) plotted as a function of the cross-RHI wind direction, in polar coordinates, for (a) Dunkerque and (b) Paris. For each site, the figure includes data from the whole period indicated in Table 1, and for all altitudes between the top of the blind zone and 200 m above the lidar. The colour scale represents the density of points, expressed as a fraction of their total number (53,667 in Dunkerque and 11,248 in Paris), in log scale.

https://doi.org/10.5194/egusphere-2025-5639
Preprint. Discussion started: 8 January 2026

3.2. Correction of the flow inclination

3.2.1. Performance of the optimization process

In this section, the optimization was performed using the lowest 500 m of the profile to define the error. Three search intervals were tested: a narrow one (–6.00° to +9.70°), a medium one (–12.00° to +19.42°) and a wide one (–18.00° to +29.12°; see Sec. S3.2 of the supplement for details about the boundary values). When the single-RHI one-dimensional inclination was optimized within the narrow search interval, the two-dimensional flow inclination could not be determined for 21.0% of the RHI pairs recorded in Paris, and 21.9 % in Dunkerque. Using the medium search interval reduced this share significantly, down to 12.1% in Paris and 11.8 % in Paris. However, extending to the wide search interval had a more limited effect, still leaving 8.3% of the RHI pairs aside on both sites, while allowing such large inclinations values is questionable. For the narrow and the medium search intervals alike, about two third of the non-optimized cases occurred between 10:00 and 18:00 UTC, confirming that it was impossible to optimize the flow inclination mainly during the convective periods, when strong turbulence made the flow inclination indiscernible.

For the RHI pairs for which the two-dimensional flow inclination was retrieved successfully, the most frequent value of the inclination angle was approximately 0.6° in Dunkerque and 1.0° in Paris, no matter the width of the search interval (Fig. S5). The peak in the two-dimensional inclination distribution did not widened significantly with the extension of the search interval (in Paris, the 67th percentile was located respectively at 1.9°, 2.4° and 2.6° for the narrow, medium and wide search intervals). However, the right tail of the distribution extended much more rapidly as the search interval was widened (in Paris, the 95th percentile was located respectively at 4.3°, 8.0° and 11.7° for the narrow, medium and wide search intervals). Flow inclinations above a few degrees did not seem realistic, so the dataset retrieved using the medium search interval was preferred to study the effect of the optimization on the TKE retrieval. No simple relationship could be found between the direction of the wind and the azimuth of the two-dimensional flow inclination (Fig. S6).

The impact of terrain inclination on the DBS or VAD technique has been regularly explored over the past 20 years, as the horizontal homogeneity assumption required in the DBS and VAD retrievals is not valid over a sloping or complex terrain (e.g. Bingöl et al., 2009; Kim et al., 2016). The detailed interpretation of the differences observed in intercomparison studies requires Computer Fluid Dynamics (CFD) simulations of the flow, especially in complex terrains (e.g. Behrens et al., 2012; Indasi et al., 2016; Kim et al., 2016). The Paris area is not a simple sloping, but smooth terrain (a map of the orography around the lidar site can be found in Cheliotis et al., 2020), so the flow inclinations obtained for this site are indeed difficult to interpret without resorting to a CFD model. In Dunkerque region, the frequent flow inclinations from the South-East can be related to the land-sea interface, as this direction is roughly perpendicular to the coastline. Nevertheless, explaining the other flow inclinations observed would, again, require CFD modeling. A study of the terrain impact on the cross-RHI reconstruction is beyond the scope of this paper, and the design of this technique itself can be expected to preserve it from bias, so the flow inclination was not studied further, but simply used as a way to optimize the TKE retrieval, to avoid contamination of the intra-layer variance due to the wind shear.

https://doi.org/10.5194/egusphere-2025-5639
Preprint. Discussion started: 8 January 2026

3.2.2. Impact on the horizontal turbulent kinetic energy

Figure 5 present the evolution of the horizontal TKE on the same day as Figure 2, showing the development of the connective PBL and the shear layers associated with the nocturnal LLJ and the breezes. Other examples of the TKE_h variability during one-day case studies in Paris are presented in Fig. S8(a) and Fig. S9(e) of the supplement. To perform a statistical validation, a first step was to assess the impact of the flow inclination optimization on the horizontal TKE retrieval, by comparing values obtained with and without the inclination (Fig. S12). Similarly to Bonin et al. (2017), data were fitted in logarithmic scale and with a unity slope, in which case the intercept b is simply equal to the average of the logarithmic ratio $\eta = \log_{10}(TKE_{RHItilt}/TKE_{RH})$ (Sec. S6 of the supplement). The 95 % confidence interval on b was assessed using the stationary-bootstrap (James et al., 2013; Politis and Romano, 1994), as it does not require assuming a model for the distribution of η. The slope values in linear scale indicated on Fig. S12 correspond to 10^b, and give the bias between the TKE_h values with and without the layers' inclination. These bias values are summarized in Table 2.

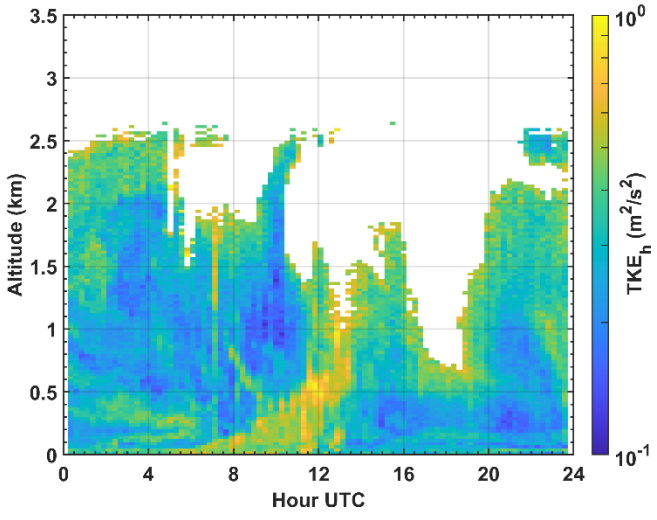

Figure 5. Time-altitude cross-section of the horizontal TKE retrieved over Dunkerque on September 9th 2023 using the cross-RHI method.

When the layers' inclination was optimized over the lowest 0.5 km of the profile, the confidence interval on the bias overlapped 1, which means that the change in the horizontal TKE was not statistically discernable. This result may seem counter intuitive as the goal of the optimization process is precisely to minimize the wind variances inside the layers, thus decrease the TKE_h values. However, the flow inclination retrieved at low altitudes may not be adapted at higher altitudes (by nighttime, for instance, there may be differences between the nocturnal PBL and the residual layer). When the optimization layer was thickened to 1.0 or 1.5 km, the bias and its confidence interval clearly fell below 1, meaning that the horizontal TKE was significantly reduced by using tilted layers, as expected. The decrease was twice more marked in Paris (–5.6 %) than in Dunkerque (–2.7 %) for the 1.5-km optimization. Indeed, larger inclination angles were retrieved in Paris (Sec. 3.2.1), so the effects of tilting the layers on the horizontal TKE retrieval were logically larger in Paris.

https://doi.org/10.5194/egusphere-2025-5639
Preprint. Discussion started: 8 January 2026

Table 2. Bias between the horizontal TKE retrieved with and without the layers' inclination optimization, expressed as the linear slope 10^b, with the associated 95 % stationary-bootstrap confidence interval. The bias was computed for different optimization layers, i.e. different values of the N_{lay} parameter. Data from the whole period and all altitudes were considered altogether.

	Paris		Dunkerque	
Optimization layer	Slope	Conf. Int.	Slope	Conf. Int.
Lowest 0.5 km	1.005	0.996 – 1.015	1.003	1.000 – 1.005
Lowest 1.0 km	0.957	0.952 – 0.963	–	–
Lowest 1.5 km	0.944	0.940 – 0.948	0.973	0.972 – 0.974

These first results suggest that the way TKE_h is affected by the layers' inclination varies with altitude. To investigate this question, the slope values were determined separately for different altitude bands, and a bias profile was constructed for the Paris site (Figure 6). The horizontal TKE was significantly reduced (confidence interval entirely below 1) within the optimization layer and slightly above, but the TKE_h actually increased at higher altitudes (up to +9 %). The horizontal TKE retrieval should therefore be limited in height, to the top of the optimization layer, so that it is tempting to extend the optimization layer in height, possibly using the full profile. However, the decrease in TKE_h at low altitudes was more pronounced when using a shallow optimization layer. For instance, in the first altitude band (0-100 m above the lidar), the drop reached –5.2 % (confidence interval –5.6 to –4.7 %) when the optimization was performed over the lowest 0.5 km (Figure 6a), but it was only –1.8 % (confidence interval –2.2 to –1.3 %) with an optimization over the lowest 1.5 km (Figure 6c). This means that the near-ground TKE_h was more efficiently corrected from the atmospheric flow inclination effects when the tilt angle was optimized also at low altitude. As pointed above, it is possible for the flow inclination to change between the different atmospheric layers, so that using a single inclination angle to reconstruct the whole TKE_h profile may be inappropriate. A possible solution is to limit the TKE_h profile to the layers of interest, for instance to the lowest few hundred meters for wind energy applications. If a full-height TKE_h profile is needed, then a composite profile should be built from several sub-profiles optimized over different layers.

https://doi.org/10.5194/egusphere-2025-5639
Preprint. Discussion started: 8 January 2026

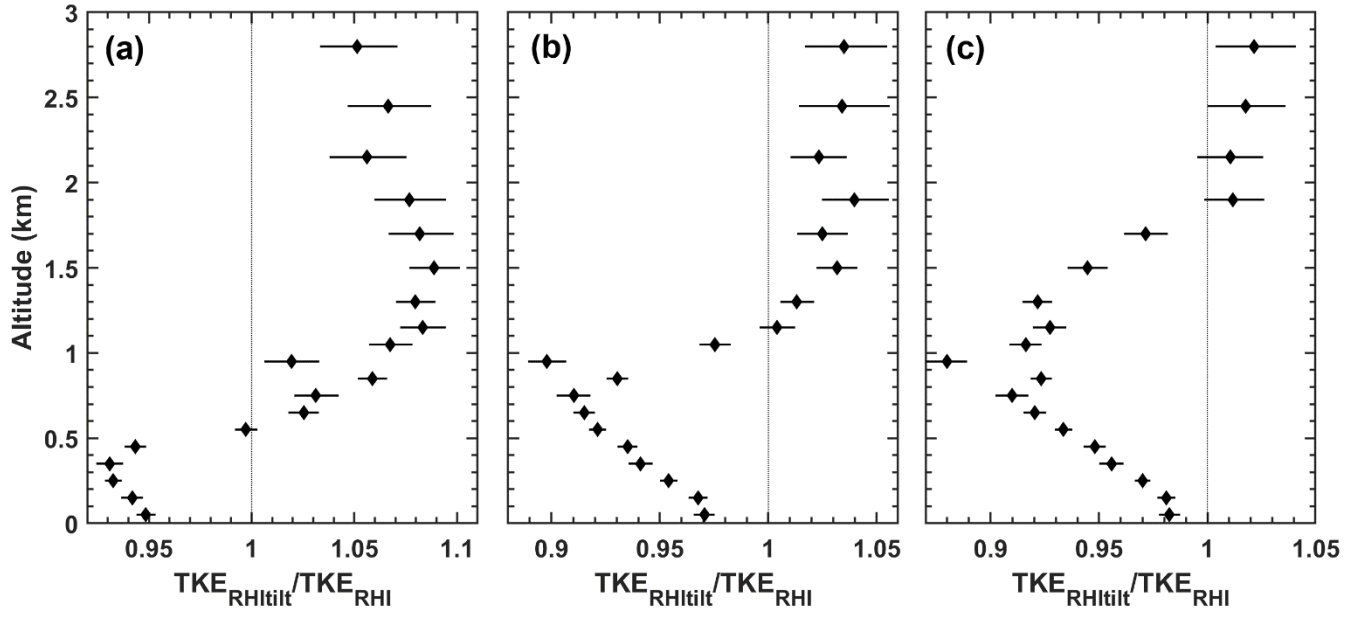

Figure 6. Vertical profile of bias between the TKE retrieved with and without the layers' inclination optimization, expressed as the linear slope 10^b (diamonds), with the 95 % stationary-bootstrap confidence interval (horizontal lines), for the site of Paris. The layers' inclination was optimized over the lowest (a) 0.5 km, (b) 1.0 km and (c) 1.5 km. Data were binned into altitude bands before fitting: 100 m-wide bands up to 1.2 km, then 200 m up to 2.0 km, and 300 m above to compensate the decreasing amount of data with altitude.

The effect of the layers' inclination on the TKE_h retrieval was relatively constant over the lowest 200 m above the lidar, then the bias decreased steadily with altitude, reaching a minimum around 1 km when the optimization layer included these altitudes (Figure 6b, c). Indeed, the flow inclination was generally little visible at low altitudes, where wind shear was limited by persistent turbulence, even by night (with the strong urban heat island in Paris, nocturnal PBL depth values stand around 200 m, even in winter; Dieudonné, 2012). On the contrary, the flow inclination had a large impact on the horizontal TKE retrieval at medium altitudes, where frequent low-level jets induce strong wind shear (Céspedes et al., 2024). The drop in TKE_h went down to –12.0 % between 0.9 and 1.0 km, which means that not taking the flow inclination into account at these altitudes would lead to a notable overestimation of the horizontal TKE. Similar results were obtained for the site of Dunkerque (Fig. S13), though the bias values were overall closer to 1 in this flatter site.

In a second step, the horizontal TKE from the cross-RHI retrieval was compared with observations from an ultrasonic anemometer (Figure 7). No anemometer was available during the Paris campaign, and there was no tall mast in Dunkerque, so the comparison bore only on the first level of the retrieval in Dunkerque. The layers' inclination angle was therefore optimized using only the lowest 500 m of the profile, for the retrieval to be the best adapted close to the ground. There was more dispersion for the TKE_h than for the wind speed values, but the Pearson correlation coefficient was still relatively high (0.69). Data were fitted in the same way as previously, and the bias indicates that the cross-RHI retrieval overestimated the TKE_h by 12.7 % (confidence interval 6.9 to 19.2 %), even with the layers' inclination optimization. The anemometer was located closer to the

https://doi.org/10.5194/egusphere-2025-5639
Preprint. Discussion started: 8 January 2026

shore than the lidar, and lidar horizontal sweeps showed that turbulence organization changes over a few hundred meters when a maritime air mass crosses the sea-land interface (Maynard, 2025), so Figure 7 was replotted selecting only the offshore or onshore wind directions (not shown). However, no significant difference was observed, so surface contrast effects were probably not responsible for the differences between the cross-RHI and the ultrasonic TKE_h values. On the other hand, as explained in Sec. 2.3.3, the first level of the lidar retrieval went from the anemometer level to 12.5 m above it, so it is possible that the lidar retrieved higher turbulence simply because it observed slightly higher. A contribution from the instrumental random errors is also likely, as there is currently no method to correct for these errors in the cross-RHI retrieval. In the absence of a tall mast equipped with ultrasonic anemometers farther from the ground, a solution would be to measure turbulence profiles with the lidar, for instance using the six-beam technique (Sathe et al., 2015). However, such observations could not fit in the lidar measurement cycle in Dunkerque, as it also included horizontal sweeps for coherent turbulent structures observations. Further intercomparison studies are therefore still needed, on sites equipped with a tall mast, or by reprogramming the lidar to perform in alternance six-beam profiles and perpendicular RHI sweeps.

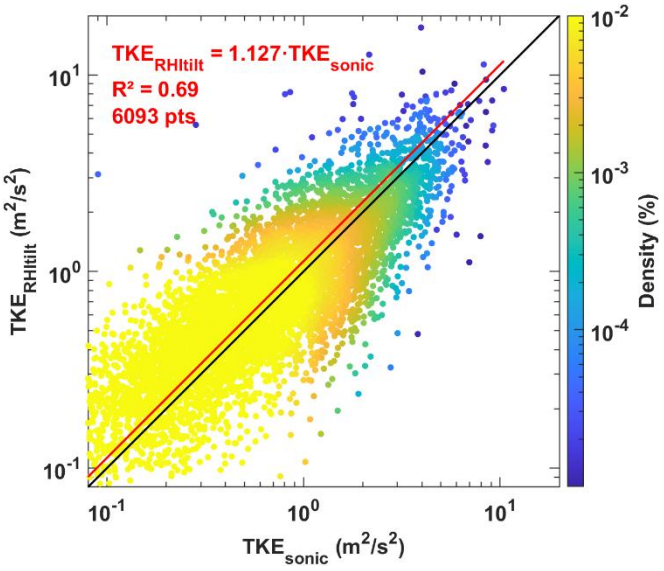

Figure 7. Scatter plot of the horizontal component of the TKE from the cross-RHI reconstruction method *vs* the ultrasonic anemometer in Dunkerque, for the whole four-month period. RHI data are from the first level of the reconstructed profile, and from the retrieval with inclined layers optimized over the first 500 m. The red line is the result of the unity-slope fit; the black line is the 1:1 line.

4. Summary and conclusions

Scanning Doppler lidars are very versatile instruments in terms of observation strategy, but in order to retrieve the horizontal wind profile, many users limit themselves to the DBS technique. Because it is pre-implemented in the lidar instruments' software, the DBS retrieval is performed online, allowing for a real-time observation of the wind profile and eliminating the need for expertise in wind reconstruction algorithms. However, the DBS leaves a blind zone of about 50 m minimum near the

https://doi.org/10.5194/egusphere-2025-5639
Preprint. Discussion started: 8 January 2026

ground, which can be detrimental when studying very low-altitude phenomena, for instance in urban or forest canopies. Moreover, turbulence makes the DBS wind profiles noisy in convective conditions, unless averaging over several tens of DBS cycles, in which case time may lack to record other types of sweeps, and the lidar periscope gears will suffer extra fatigue. Another horizontal wind reconstruction method was introduced in the 2000's, based on pairs of perpendicular vertical sweeps of the RHI type, but this so called cross-RHI technique was seldom reused since then, and always limited to low-elevation beams and thus, short-range wind profiles. This paper and it supplement thus provided a more detailed description of the cross-RHI horizontal wind reconstruction process, including a filtering method to remove range-folded echoes from clouds, and a technique to account for the atmospheric flow inclination. For this latter purpose, the tilt angle of the binning layers used in the retrieval process was optimized so as to minimize the intra-layer wind speed variance, i.e. the horizontal components of the TKE, thus eliminating the TKE overestimation due to wind shear.

The cross-RHI method was applied to produce full-height wind profiles, and compared with standard DBS wind profiles. The case studies presented highlighted the ability of the cross-RHI technique to operate with lower aerosol loads than the DBS, to produce smoother profiles in convective conditions, and to efficiently filter out cloud echoes while enabling to observe very low-latitude phenomena. A statistical intercomparison was also performed, using six months of observations in total: four months from an industrial harbor city in a flat coastal area (Dunkerque), and two months from a megacity at a more hilly continental site (Paris). A very good agreement was observed between horizontal wind speed values retrieved using both methods, with Pearson correlation coefficients around 0.85 below a 200-m altitude on both sites. In average, the cross-RHI reconstruction tended to produce slightly lower speed values than the DBS retrieval, but the fitting slope of 0.93 was actually dragged down by a small share of points that appeared grossly overestimated by the DBS due to cloud echoes. The wind direction values exhibited more dispersion, though the difference remained lower than 10° for 83 % of the measurement points located below 200 m in Dunkerque (where 10 consecutive DBS cycles were averaged) and 62 % in Paris (using a single DBS cycle). The agreement between both retrieval methods steadily increased with altitude, as strong range-folded echoes from liquid-water clouds mainly occurred in the lower part of the DBS profile. The wind speed values thus exhibited correlation coefficients and slopes closer to one (both around 0.97) for altitudes above 1 km, while the share of points having a direction error below 10° reached 91 % in Dunkerque and 82 % in Paris. This work thus demonstrated that the cross-RHI wind reconstruction method can be used to retrieve full-height wind profiles without limiting the sweeps to low-elevation beams.

The inclination of the binning layers could be optimized successfully for 88 % of the cross-RHI pairs on both sites, whereas about two-third of the non-optimized cases actually corresponded to daytime convective conditions, under which defining an inclination of the atmospheric flow was impossible. The most frequent two-dimensional tilt angles were typically 1.0° in Paris and 0.6° on the flatter site of Dunkerque, but the direction of the steepest slope did not exhibit a simple relationship with the orographic features. The effect of the layers' inclination on the horizontal TKE values could reach down to –12 % but depended strongly on the altitude of the observations and on the altitude band chosen for the optimization. The horizontal TKE decreased as expected within the altitude band upon which it was minimized, but actually increased above, as the inclination angle retrieved in the lower convective PBL or nocturnal PBL was not adapted to the flow in the residual layer of free troposphere.

https://doi.org/10.5194/egusphere-2025-5639
Preprint. Discussion started: 8 January 2026

When the optimization was performed on the lowest 0.5 km of the profile, to favor the retrieval in the lower PBL, the near-ground horizontal TKE was, in average, decreased by 5.2 % in Paris. Finally, a comparison with observations from a near-ground ultrasonic anemometer in Dunkerque showed that the cross-RHI retrieval overestimated the horizontal TKE by about 13 % despite the flow inclination optimization, though the shares of this overestimation due to the slight difference in altitude between the two instruments and to random instrumental errors in the lidar observations are not known.

Compared to the six-beam technique, that is becoming the new standard to measure the turbulence profile, the cross-RHI technique has the advantage to fill in the blind zone near the ground, while offering a more stable inversion process (negative variance values can sometimes come out of the matrixial inversion involved in the six-beam retrieval, in which case data must be discarded). Moreover, as long as the six-beam measurement scenario will not be pre-implemented in the lidar software, each beam of the cycle will result in a separate small data file, which saturates the instrument memory faster than recording DBS.

Further development of the cross-RHI method will include the combination of several flow inclination angles, optimized over different altitude bands, in order to build composite horizontal TKE profiles. The Doppler lidar in Dunkerque was also reprogrammed for the measurement cycle to include the fixed vertical shots necessary to retrieve the complete TKE, and a second, almost colocalized instrument recorded simultaneously six-beam profiles and PPI sweeps for the double-VAD turbulence retrieval technique. Eight months of data have been gathered in this configuration, that will soon be exploited to validate the cross-RHI TKE retrieval farther above ground. By providing the software used in this study, we also hope to make cross-RHI wind reconstruction method more widely available in the community, and encourage its implementation by the Doppler lidar manufacturers in the near future.

Data availability statement

The Doppler lidar data from the Paris site (DBS wind profiles and RHI radial wind) along with the Matlab® software used to reconstruct the wind profiles from the RHI sweeps are available from the Zenodo platform (Dieudonné et al., 2025). Data are provided in the Matlab® binary format used by the provided processing codes, and in the NetCDF4 open format. The Doppler lidar data from the Dunkerque site is available from the first author, upon request.

Author contributions

HD developed the scientific programs for the funding of the Doppler lidars. PA, MF, ED, HD and PH deployed the instruments on the field and ensured their monitoring and maintenance. ED developed the wind reconstruction software, with contributions of AS for the layer inclination optimization part. ED and PH respectively processed the Paris and Dunkerque observations. ED wrote the original manuscript, with all authors contributing to the proofreading.

https://doi.org/10.5194/egusphere-2025-5639
Preprint. Discussion started: 8 January 2026

Competing interests

The authors declare no conflict of interest.

Acknowledgements

The authors thank Pr. François Ravetta, from Sorbonne University, who coordinated the VEGILOT campaign in Paris. Experiments presented in this paper were carried out using the CALCULCO computing platform, supported by SCoSI/ULCO (*Service COmmun du Système d'Information de l'Université du Littoral Côte d'Opale*).

Financial support

The Doppler lidars were funded by the regional council of the *Région Hauts-de-France*, the French Ministry of Higher Education and Research (*Ministère de l'Enseignement Supérieur et de la Recherche*) and the European Fund for Regional Economic Development (ERDF) through the successive CPER programs IRENI, IRENE and ECRIN. Mission fees were funded by the CaPPA Labex, a project funded by the French National Research Agency (ANR), through the PIA (*Programme d'Investissement d'Avenir*) under the contract ANR-11-LABX-0005-01, and through the *Région Hauts-de-France* and the ERDF. Pauline Haezebrouck's Ph.D. grant was co-funded by the *Région Hauts-de-France* and the conurbation authority (*Pôle Métropolitain de la Côte d'Opale*), while Perrine Maynard's Ph.D. grant was co-funded by the *Région Hauts-de-France* and the CaPPA Labex.

References

Augustin, P., Billet, S., Crumeyrolle, S., Deboudt, K., Dieudonné, E., Flament, P., Fourmentin, M., Guilbaud, S., Hanoune, B., Landkocz, Y., Méausoone, C., Roy, S., Schmitt, F. G., Sentchev, A., and Sokolov, A.: Impact of Sea Breeze Dynamics on Atmospheric Pollutants and Their Toxicity in Industrial and Urban Coastal Environments, Remote Sens., 12, 648, https://doi.org/10.3390/rs12040648, 2020.

Baidar, S., Wagner, T. J., Turner, D. D., and Brewer, W. A.: Using optimal estimation to retrieve winds from velocity-azimuth display (VAD) scans by a Doppler lidar, Atmos. Meas. Tech., 16, 3715–3726, https://doi.org/10.5194/amt-16-3715-2023, 2023.

Banta, R. M., Newsom, R. K., Lundquist, J. K., Pichugina, Y. L., Coulter, R. L., and Mahrt, L.: Nocturnal Low-Level Jet Characteristics Over Kansas During Cases-99, Bound.-Lay. Meteorol., 105, 221–252, https://doi.org/10.1023/A:1019992330866, 2002.

https://doi.org/10.5194/egusphere-2025-5639
Preprint. Discussion started: 8 January 2026

Banta, R. M., Pichugina, Y. L., and Brewer, W. A.: Turbulent Velocity-Variance Profiles in the Stable Boundary Layer Generated by a Nocturnal Low-Level Jet, J. Atmos. Sci., 63, 2700–2719, https://doi.org/10.1175/JAS3776.1, 2006.

Behrens, P., O'Sullivan, J., Archer, R., and Bradley, S.: Underestimation of Monostatic Sodar Measurements in Complex Terrain, Bound.-Lay. Meteorol., 143, 97–106, https://doi.org/10.1007/s10546-011-9665-6, 2012.

Benjamin, S. G., Schwartz, B. E., Szoke, E. J., and Koch, S. E.: The Value of Wind Profiler Data in U.S. Weather Forecasting, B. Am. Meteorol. Soc., 85, 1871–1886, https://doi.org/10.1175/BAMS-85-12-1871, 2004.

Bingöl, F., Mann, J., and Foussekis, D.: Conically scanning lidar error in complex terrain, Meteorol. Z., 18, 189–195, https://doi.org/10.1127/0941-2948/2009/0368, 2009.

Bonin, T. A., Choukulkar, A., Brewer, W. A., Sandberg, S. P., Weickmann, A. M., Pichugina, Y. L., Banta, R. M., Oncley, S. P., and Wolfe, D. E.: Evaluation of turbulence measurement techniques from a single Doppler lidar, Atmos. Meas. Tech., 10, 3021–3039, https://doi.org/10.5194/amt-10-3021-2017, 2017.

Brent, R. P.: Algorithms for minimization without derivatives, Prentice Hall, Inc., Englewood Cliffs (NJ), 1973.

Browning, K. A. and Wexler, R.: The Determination of Kinematic Properties of a Wind Field Using Doppler Radar, J. Appl. Meteorol. Clim., 7, 105–113, https://doi.org/10.1175/1520-0450(1968)007%253C0105:TDOKPO%253E2.0.CO;2, 1968.

Calhoun, R., Heap, R., Princevac, M., Newsom, R., Fernando, H., and Ligon, D.: Virtual Towers Using Coherent Doppler Lidar during the Joint Urban 2003 Dispersion Experiment, J. Appl. Meteorol. Clim., 45, 1116–1126, https://doi.org/10.1175/JAM2391.1, 2006.

Céspedes, J.: Summertime nocturnal Low-Level Jet in the Paris region: interactions with the urban heat and surface characteristics, Ph.D. thesis, Institut Polytechnique de Paris, Palaiseau (France), 137 pp., 2024.

Céspedes, J., Kotthaus, S., Preissler, J., Toupoint, C., Thobois, L., Drouin, M.-A., Dupont, J.-C., Faucheux, A., and Haeffelin, M.: The Paris low-level jet during PANAME 2022 and its impact on the summertime urban heat island, Atmospheric Chemistry and Physics, 24, 11477–11496, https://doi.org/10.5194/acp-24-11477-2024, 2024.

Chazette, P., Flamant, C., Sodemann, H., Totems, J., Monod, A., Dieudonné, E., Baron, A., Seidl, A., Steen-Larsen, H. C., Doira, P., Durand, A., and Ravier, S.: Experimental investigation of the stable water isotope distribution in an Alpine lake environment (L-WAIVE), Atmos. Chem. Phys., 21, 10911–10937, https://doi.org/10.5194/acp-21-10911-2021, 2021.

Cheliotis, I., Dieudonné, E., Delbarre, H., Sokolov, A., Dmitriev, E., Augustin, P., and Fourmentin, M.: Detecting turbulent structures on single Doppler lidar large datasets: an automated classification method for horizontal scans, Atmos. Meas. Tech., 13, 6579–6592, https://doi.org/10.5194/amt-13-6579-2020, 2020.

https://doi.org/10.5194/egusphere-2025-5639
Preprint. Discussion started: 8 January 2026

Cheliotis, I., Dieudonné, E., Delbarre, H., Sokolov, A., Dmitriev, E., Augustin, P., Fourmentin, M., Ravetta, F., and Pelon, J.: Properties of coherent structures over Paris: a study based on an automated classification method for Doppler lidar observations, J. Appl. Meteorol. Clim., 60, 1545–1559, https://doi.org/10.1175/JAMC-D-21-0014.1, 2021.

Chong, M., Georgis, J.-F., Bousquet, O., Brodzik, S. R., Burghart, C., Cosma, S., Germann, U., Gouget, V., Houze, R. A., James, C. N., Prieur, S., Rotunno, R., Roux, F., Vivekanandan, J., and Zeng, Z.-X.: Real-Time Wind Synthesis from Doppler Radar Observations during the Mesoscale Alpine Programme, B. Am. Meteorol. Soc., 81, 2953–2962, 2000.

Clark, W. L., Green, J. L., and Warnock, J. M.: Estimating meteorological wind vector components from monostatic Doppler radar measurements: A case study, Radio Sci., 20, 1207–1213, https://doi.org/10.1029/RS020i006p01207, 1985.

Crumeyrolle, S., Augustin, P., Rivellini, L.-H., Choël, M., Riffault, V., Deboudt, K., Fourmentin, M., Dieudonné, E., Delbarre, H., Derimian, Y., and Chiapello, I.: Aerosol variability induced by atmospheric dynamics in a coastal area of Senegal, North-Western Africa, Atmos. Environ., 203, 228–241, https://doi.org/10.1016/j.atmosenv.2019.01.041, 2019.

Davies-Jones, R. P.: Dual-Doppler Radar Coverage Area as a Function of Measurement Accuracy and Spatial Resolution, J. Appl. Meteorol. Clim., 18, 1229–1233, https://doi.org/10.1175/1520-0450-18.9.1229, 1979.

Dieudonné, E.: Analyse multi-instrumentale de l'influence de la variabilité de la hauteur de couche limite sur la distribution verticale des oxydes d'azote en région parisienne, Ph.D. thesis, Université Paris VI Pierre et Marie Curie, Paris, France, 229 pp., 2012.

Dieudonné, E., Delbarre, H., Sokolov, A., Ebojie, F., Augustin, P., and Fourmentin, M.: Characteristics of the low-level jets observed over Dunkerque (North Sea French coast) using 4 years of wind lidar data, Q. J. R. Meteor. Soc., 149, 1745–1768, https://doi.org/10.1002/qj.4480, 2023.

Dieudonné, E., Haezebrouck, P., Maynard, P., Sokolov, A., Delbarre, H., Augustin, P., and Fourmentin, M.: Data and codes associated with "Doppler lidar wind profiling: long-term assessment of the perpendicular vertical sweeps reconstruction method" (1), https://doi.org/10.5281/zenodo.17598381, 2025.

Dolatabadi, A., Abdeltawab, H., and Mohamed, Y. A.-R. I.: Deep Spatial-Temporal 2-D CNN-BLSTM Model for Ultrashort-Term LiDAR-Assisted Wind Turbine's Power and Fatigue Load Forecasting, IEEE T. Ind. Inform., 18, 2342–2353, https://doi.org/10.1109/TII.2021.3097716, 2022.

Eberhard, W. L., Cupp, R. E., and Healy, K. R.: Doppler Lidar Measurement of Profiles of Turbulence and Momentum Flux, J. Atmos. Ocean Tech., 6, 809–819, https://doi.org/10.1175/1520-0426(1989)006%253C0809:DLMOPO%253E2.0.CO;2, 1989.

Emeis, S., Harris, M., and Banta, R. M.: Boundary-layer anemometry by optical remote sensing for wind energy applications, Meteorol. Z., 16, 337–347, https://doi.org/10.1127/0941-2948/2007/0225, 2007.

https://doi.org/10.5194/egusphere-2025-5639
Preprint. Discussion started: 8 January 2026

Forsythe, G. E., Malcolm, M. A., and Moler, C. B.: Computer Methods for Mathematical Computations, Prentice Hall, Inc., Englewood Cliffs (NJ), 1976.

Hong Kong Observatory: Wiindshear and Turbullence in Hong Kong - information for pilots, Hong Kong Special Administrative Region Government, Hong Kong, 2019.

Indasi, V. S., Lynch, M., McGann, B., Yu, F., Jeanneret, F., and Sutton, J.: WAsP model performance verification using lidar data, Int. J. Energy Environ. Eng., 7, 105–113, https://doi.org/10.1007/s40095-015-0189-6, 2016.

James, G., Witten, D., Hastie, T., and Tibshirani, R.: An Introduction to Statistical Learning, Springer, New York, NY, https://doi.org/10.1007/978-1-4614-7138-7, 2013.

Kim, D., Kim, T., Oh, G., Huh, J., and Ko, K.: A comparison of ground-based LiDAR and met mast wind measurements for wind resource assessment over various terrain conditions, J. Wind Eng. Ind. Aerod., 158, 109–121, https://doi.org/10.1016/j.jweia.2016.09.011, 2016.

Liu, B., Guo, J., Gong, W., Shi, L., Zhang, Y., and Ma, Y.: Characteristics and performance of wind profiles as observed by the radar wind profiler network of China, Atmos. Meas. Tech., 13, 4589–4600, https://doi.org/10.5194/amt-13-4589-2020, 2020.

Maynard, P.: Télédétection des structures turbulentes cohérentes dans la couche de surface atmosphérique : apport de l'apprentissage supervisé, Ph.D. thesis, Université du Littoral Côte d'Opale, Dunkerque (France), 234 pp., 2025.

Maynard, P., Dieudonne, E., Sokolov, A., Delbarre, H., Augustin, P., Fourmentin, M., and Dmitriev, E.: Exploring the level of organization of turbulent coherent structures in the atmospheric surface layer through supervised classification of Doppler lidar observations, J. Geophys. Res.: Mach. Learn. Comput., 2, e2025JH000652, https://doi.org/10.1029/2025JH000652, 2025.

Nash, J. and Oakley, T. J.: Development of COST 76 wind profiler network in Europe, Phys. Chem. Earth Pt. B, 26, 193–199, https://doi.org/10.1016/S1464-1909(00)00239-2, 2001.

Newsom, R. K., Ligon, D., Calhoun, R., Heap, R., Cregan, E., and Princevac, M.: Retrieval of Microscale Wind and Temperature Fields from Single- and Dual-Doppler Lidar Data, J. Appl. Meteorol. Clim., 44, 1324–1345, https://doi.org/10.1175/JAM2280.1, 2005.

Politis, D. N. and Romano, J. P.: The Stationary Bootstrap, Journal of the American Statistical Association, 89, 1303–1313, https://doi.org/10.1080/01621459.1994.10476870, 1994.

Sathe, A. and Mann, J.: Measurement of turbulence spectra using scanning pulsed wind lidars, Journal of Geophysical Research: Atmospheres, 117, https://doi.org/10.1029/2011JD016786, 2012.

Sathe, A., Mann, J., Vasiljevic, N., and Lea, G.: A six-beam method to measure turbulence statistics using ground-based wind lidars, Atmos. Meas. Tech., 8, 729–740, https://doi.org/10.5194/amt-8-729-2015, 2015.

https://doi.org/10.5194/egusphere-2025-5639
Preprint. Discussion started: 8 January 2026

Shun, C. M. and Chan, P. W.: Applications of an Infrared Doppler Lidar in Detection of Wind Shear, J. Atmos. Ocean Tech., 25, 637–655, https://doi.org/10.1175/2007JTECHA1057.1, 2008.

Smith, T. L. and Benjamin, S. G.: Impact of Network Wind Profiler Data on a 3-h Data Assimilation System, B. Am. Meteorol. Soc., 74, 801–808, https://doi.org/10.1175/1520-0477(1993)074%253C0801:IONWPD%253E2.0.CO;2, 1993.

Theuer, F., van Dooren, M. F., von Bremen, L., and Kühn, M.: Minute-scale power forecast of offshore wind turbines using long-range single-Doppler lidar measurements, Wind. Energ. Sci., 5, 1449–1468, https://doi.org/10.5194/wes-5-1449-2020, 2020.

Thobois, L., Cariou, J. P., and Gultepe, I.: Review of Lidar-Based Applications for Aviation Weather, Pure Appl. Geophys., 176, 1959–1976, https://doi.org/10.1007/s00024-018-2058-8, 2019.

Wakimoto, R. M., Murphey, H. V., Browell, E. V., and Ismail, S.: The "Triple Point" on 24 May 2002 during IHOP. Part I: Airborne Doppler and LASE Analyses of the Frontal Boundaries and Convection Initiation, Mon. Weather Rev., 134, 231–250, https://doi.org/10.1175/MWR3066.1, 2006.

Wang, C., Chen, Y., Chen, M., and Shen, J.: Data assimilation of a dense wind profiler network and its impact on convective forecasting, Atmospheric Research, 238, 104880, https://doi.org/10.1016/j.atmosres.2020.104880, 2020.

Weber, B. L., Wuertz, D. B., Strauch, R. G., Merritt, D. A., Moran, K. P., Law, D. C., Kamp, D. van de, Chadwick, R. B., Ackley, M. H., Barth, M. F., Abshire, N. L., Miller, P. A., and Schlatter, T. W.: Preliminary Evaluation of the First NOAA Demonstration Network Wind Profiler, J. Atmos. Ocean Tech., 7, 909–918, https://doi.org/10.1175/1520-0426(1990)007%253C0909:PEOTFN%253E2.0.CO;2, 1990.